

Supporting Information

High-speed AFM imaging reveals DNA capture and loop extrusion dynamics by cohesin-NIPBL

Parminder Kaur^{1,2,*}, Xiaotong Lu³, Qi Xu^{4,5}, Elizabeth Marie Irvin⁶, Colette Pappas⁷,
Hongshan Zhang^{8,9}, Ilya J. Finkelstein^{8,9}, Zhubing Shi^{4,5}, Yizhi Jane Tao³, Hongtao Yu^{4,5},
Hong Wang^{1,2,6,*}

¹Physics Department, ²Center for Human Health and the Environment, ⁶Toxicology
Program, ⁷Biological Sciences, North Carolina State University, Raleigh, NC, USA

³Department of BioSciences, Rice University, Houston, TX, USA

⁴Westlake Laboratory of Life Sciences and Biomedicine, ⁵School of Life Sciences, Westlake
University, Hangzhou, Zhejiang Province, P.R. China

⁸Department of Molecular Biosciences, ⁹Institute for Cellular and Molecular Biology,
University of Texas at Austin, Austin, TX, USA

Video S1. HS-AFM video showing dynamics of the WT cohesin^{SA1}-NIPBL^c and extension of the arm-hinge domain to capture a DNA segment in proximity (4 mM ATP). Related to Figure 3B.

Video S2. HS-AFM video showing that a DNA-bound WT cohesin^{SA1}-NIPBL^c complex captures a DNA segment in proximity through the arm-hinge domain and initiates a DNA loop (4 mM ATP). Related to Figure 4 (II to VII).

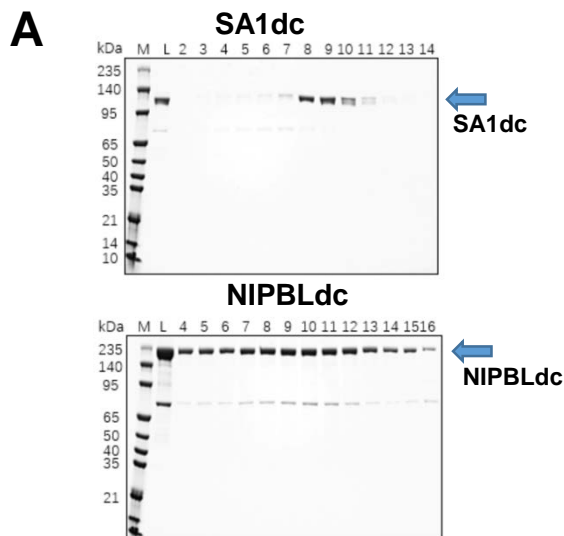
Video S3. HS-AFM video showing dynamics of cohesin^{SA1}-NIPBL^c ATPase mutant and diffusion on DNA through short protrusions (4 mM ATP). Related to Figures 5A and S5.

Video S4. HS-AFM video demonstrating diffusion on DNA through short protrusions and arm extension by the cohesin^{SA1}-NIPBL^c ATPase mutant (4 mM ATP). Related to Figure 5B.

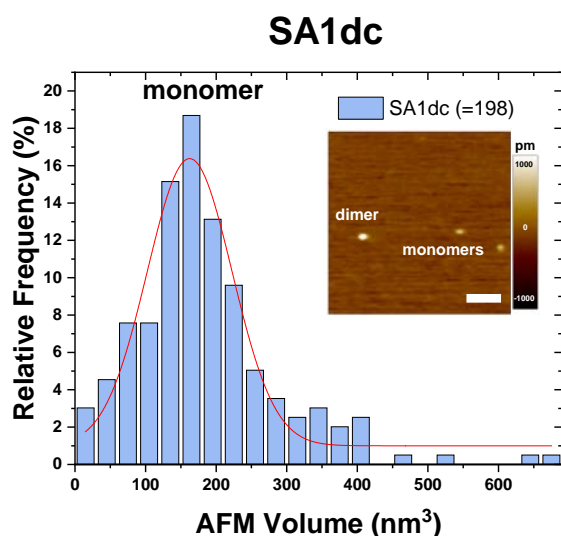
Video S5. HS-AFM video showing DNA capture by the cohesin^{SA1}-NIPBL^c ATPase mutant through arm extension (4 mM ATP). Related to Figure 5C.

Video S6. HS-AFM video showing DNA loop extrusion by WT cohesin^{SA1}-NIPBL^c (4 mM ATP). Related to Figure 7C.

Video S7. HS-AFM video showing DNA loop extrusion by WT cohesin^{SA1}-NIPBL^c (4 mM ATP). Related to Figure 7D.



B



C

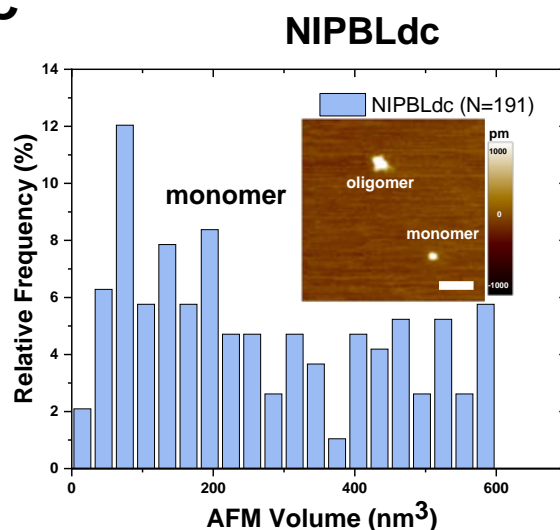


Figure S1. AFM volume analysis of SA1dc and NIPBLdc. A, SDS-PAGE of purified SA1dc and NIPBLdc. M: molecular marker. L: load. Numbers are fractions from the last FPLC purification step. B and C, Histograms of AFM volumes of SA1dc (B) and NIPBLdc (C, $<600 \text{ nm}^3$). The red line represents Gaussian fit to the data with the peak centered at $162 \text{ nm}^3 \pm 120 \text{ nm}^3$ ($R^2 > 0.90$) for SA1dc. Based on the peak, the estimation of the molecular weight is 133 KDa for SA1dc, which is close to monomers. This estimation is based on a previously established calibration curve: $V (\text{nm}^3) = 1.45 \text{ MW} - 21.57$, where V is AFM volume and MW is molecular weight (Kaur et al. Scientific Reports, 2016). Inserts show example AFM images. The complexes with volumes greater than 300 nm^3 are treated as dimers and higher-order complexes. XY scale bar = 100 nm .

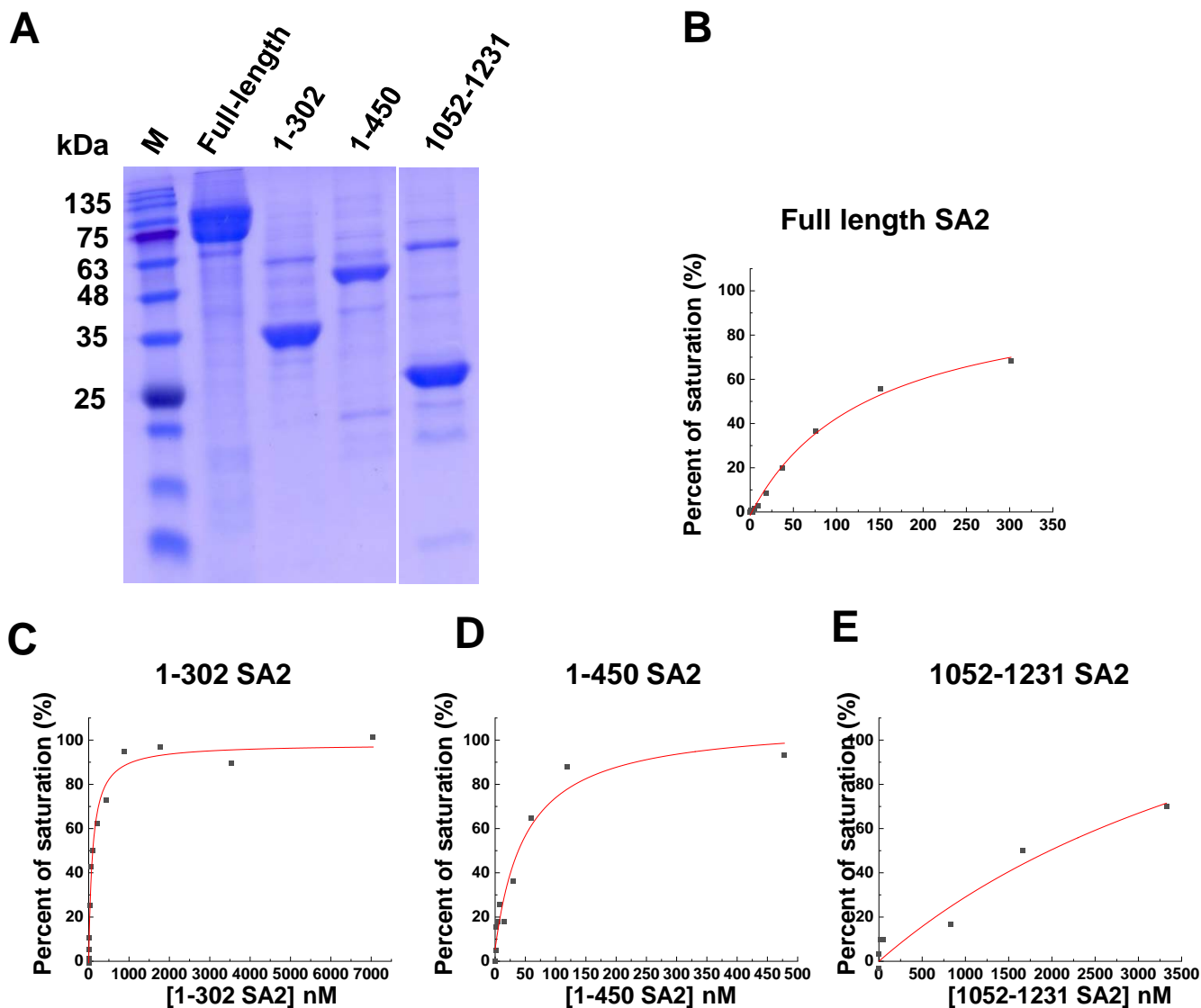


Figure S2. DNA binding by the full-length and truncation mutants of SA2. A, SDS-PAGE of the SA2 full length (1-1231 AAs), 1-302 AAs, 1-450 AAs, and 1052-1231 AAs. M: Molecular weight marker. The picture is cut from the same gel. B to E, Binding of the full length (B), 1-302 (C), 1-450 (D), and 1052-1231 (E) SA2 to 45 bp dsDNA measured by fluorescence anisotropy. dsDNA is labeled with Alexa 488. The data were fitted to the law of mass action (red lines, $R^2 > 0.9$).

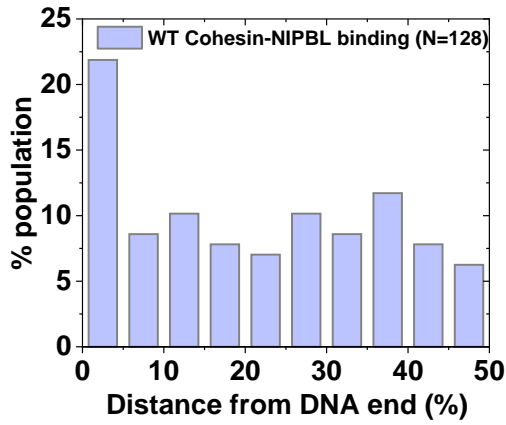
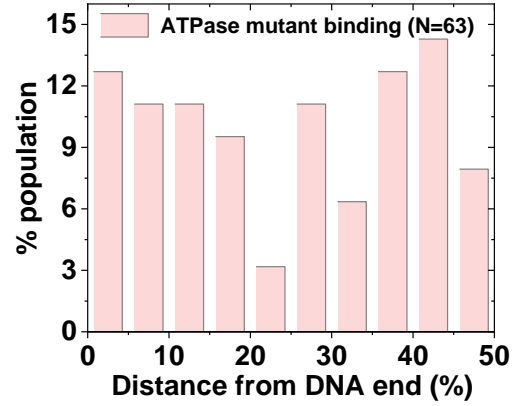
A**B**

Figure S3. DNA binding position distributions of WT and ATPase mutant cohesin^{SA1}-NIPBL^c on linear dsDNA. A and B, Position distributions of WT (A) and ATPase mutant (B) cohesin^{SA1}-NIPBL^c on a linear dsDNA substrate (5.19 kb). Two independent experiments in the presence of 2.5 mM ATP.

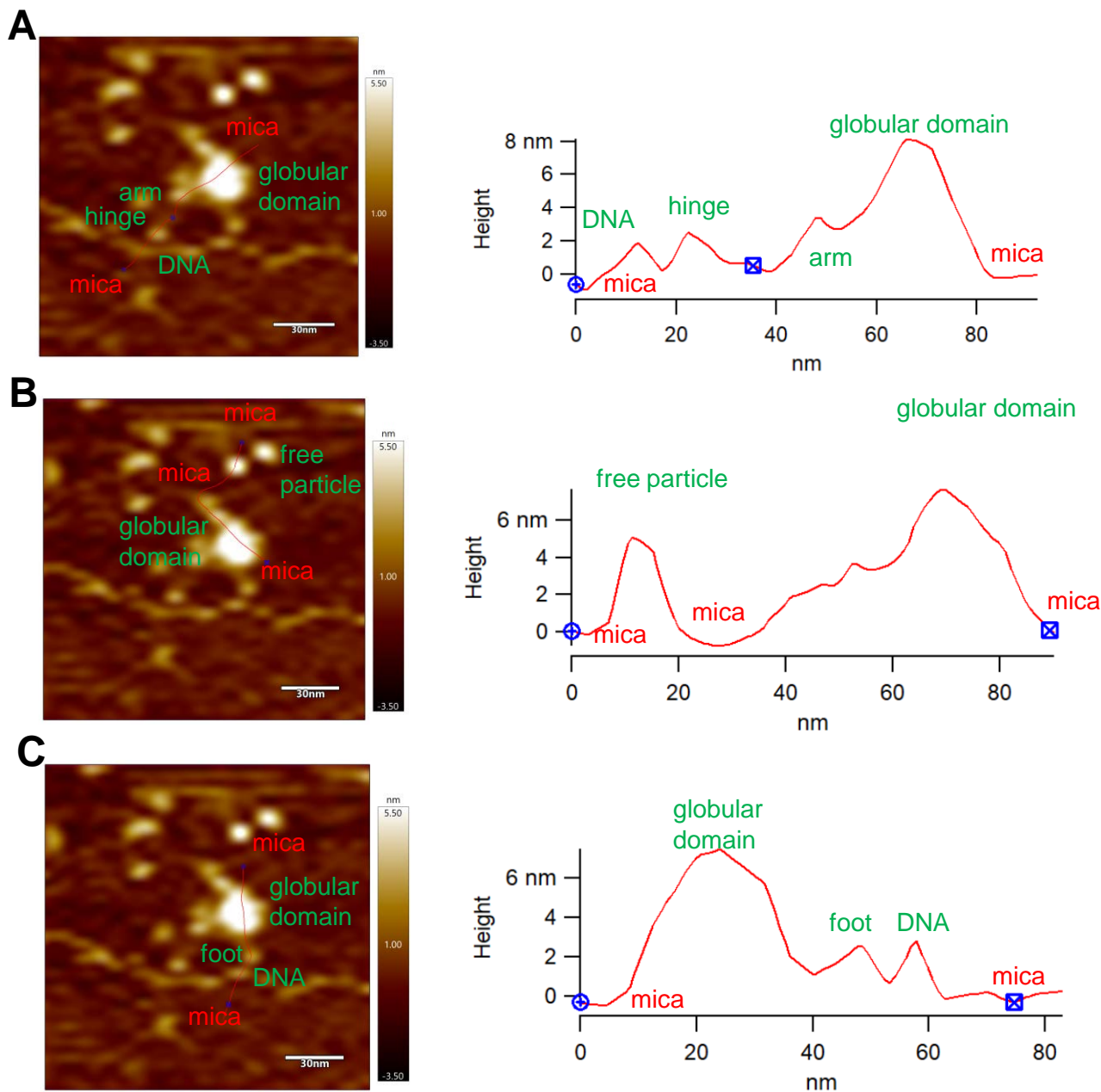


Figure S4. AFM height profile analysis showing hinge contacting DNA (A), a free particle (B), and foot connected to the globular domain contacting the DNA (C). Left panels: AFM images with the cross-sectional analysis lines in red and structural features labeled. Right panels: Cross-sectional analysis (height profile, red lines) with structural features labeled. Figures S4A-4C are re-use of the panel IV from Figure 3B for showing the height profiles at different regions.

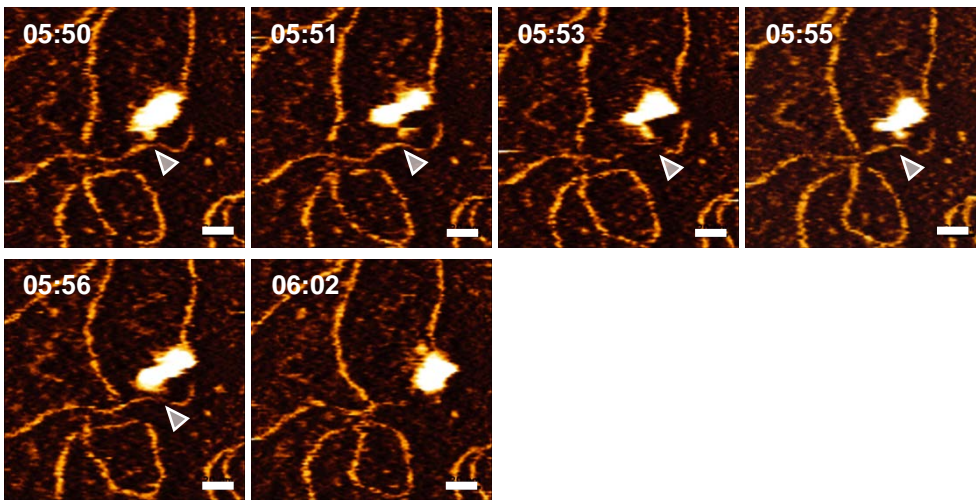


Figure S5. Time-lapse HS-AFM images of cohesin^{SA1}-NIPBL^c ATPase mutant walking (diffusion) on DNA through short protrusions. XY scale bar = 20 nm. Also see **Video S3**. Observation times are in continuation of Figure 5A for the same molecules. gray arrow: foot. Time: min:s.

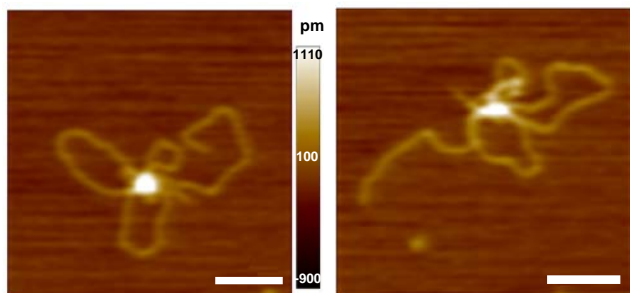
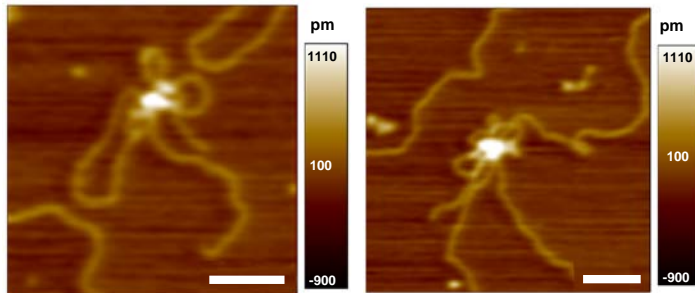
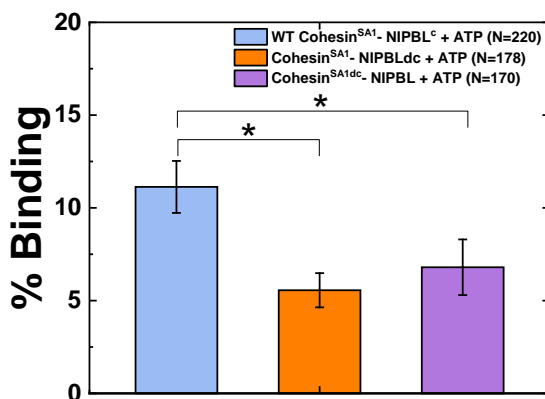
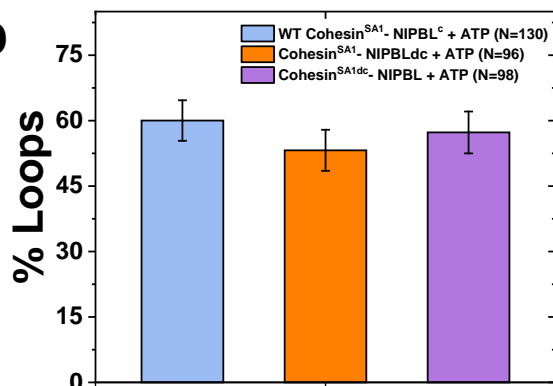
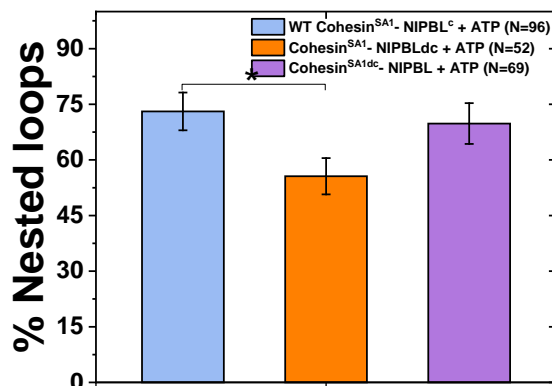
A**Cohesin^{SA1dc}-NIPBL****B****Cohesin^{SA1}-NIPBLdc****C****D****E**

Figure S6: DNA binding and loop formation mediated by cohesin-NIPBL missing the C-terminal domain of either SA1 or NIPBL. *A* and *B*, Representative AFM images of DNA loops mediated by cohesin^{SA1dc}-NIPBL (*A*) and cohesin^{SA1}-NIPBLdc (*B*) in the absence of ATP. Cohesin^{SA1}-NIPBL: 30 nM. DNA (5.19 kb): 6 nM. XY scale bar = 100 nm. *C* to *E*, Quantification of the percentages of DNA molecules bound with cohesin-NIPBL molecules (*C*), DNA loops (*D*), and nested loops out of total DNA loops mediated by WT, cohesin^{SA1dc}-NIPBL, and cohesin^{SA1}-NIPBLdc complexes. Error bars: SD. At least 3 experiments for each condition. * $p < 0.05$ based on Student's t-test. The data for WT cohesin^{SA1}-NIPBL^c is from a different batch of protein compared to the data presented in Figure 6.

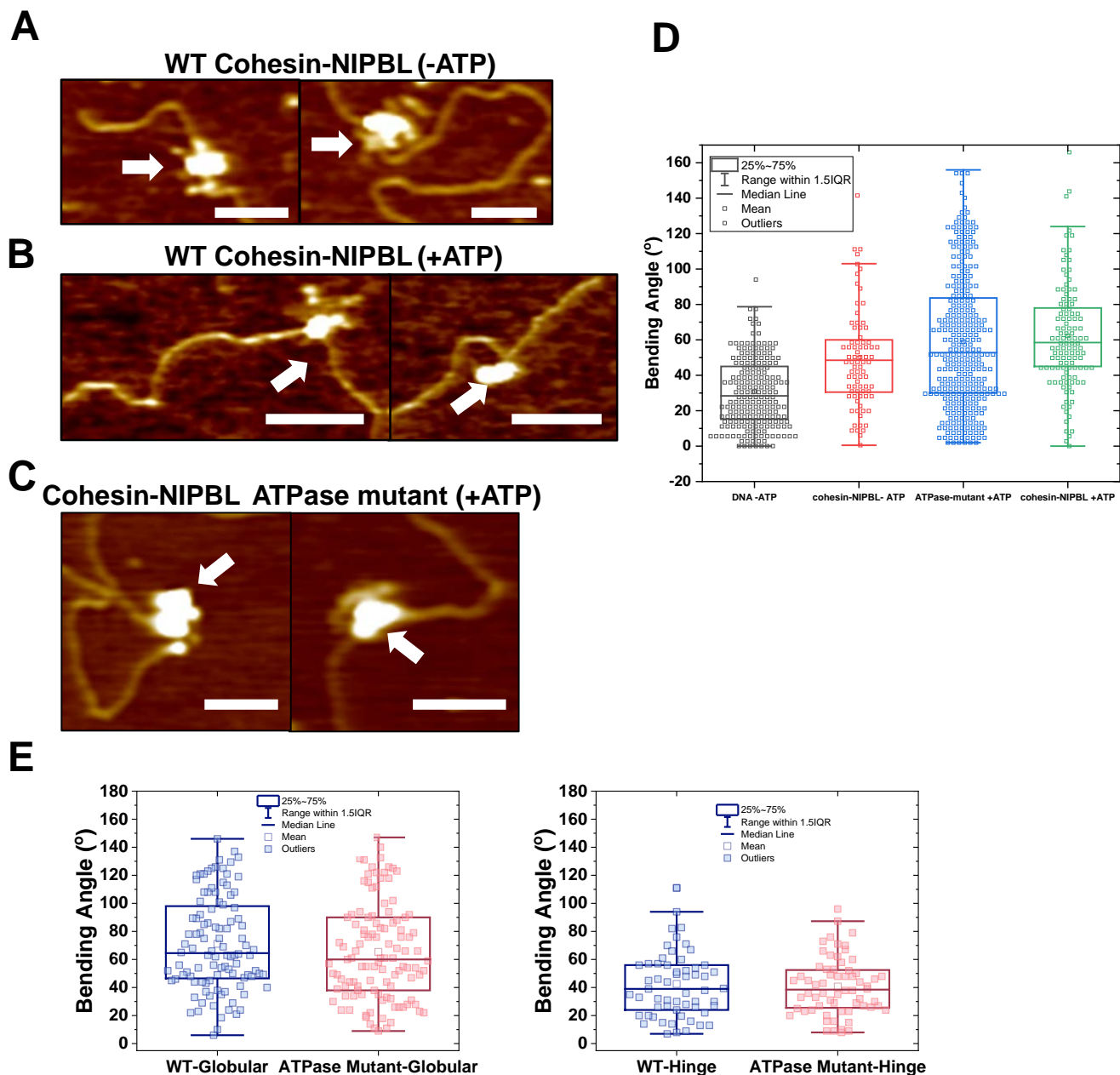


Figure S7. Cohesin^{SA1}-NIPBL^c binding induces DNA bending. A to C, Representative AFM images of WT cohesin^{SA1}-NIPBL^c in the absence (A), or presence of ATP (+2.5 mM, B), and cohesin^{SA1}-NIPBL^c ATPase mutant (+2.5 mM ATP, C) with dsDNA (5.19 kb). White arrows point to protein-DNA complexes. XY scale bar = 100 nm. D, DNA bending angles induced by the WT and ATPase mutant of cohesin^{SA1}-NIPBL^c on dsDNA. DNA bending angles: 27.5° (± 26°) for DNA_{+ATP} (N=149), 43.7° (± 20.5°) for DNA_{WT-ATP} (N=80), 57.2° (± 27.6°) for DNA_{WT+ATP} (N=116), and 47.3° (± 41.0°) for DNA_{ATPase mutant+ATP} (N=298). E, DNA bending angles induced by the globular domain (left panel) of the WT (71.2° ± 33.6°, N=104) and ATPase mutant (65.4° ± 34.6°, N=111), and the hinge domain (right panel) of WT (42.6° ± 24.4°, N=59) and ATPase mutant (40.7° ± 20.3°, N=104) cohesin^{SA1}-NIPBL^c.

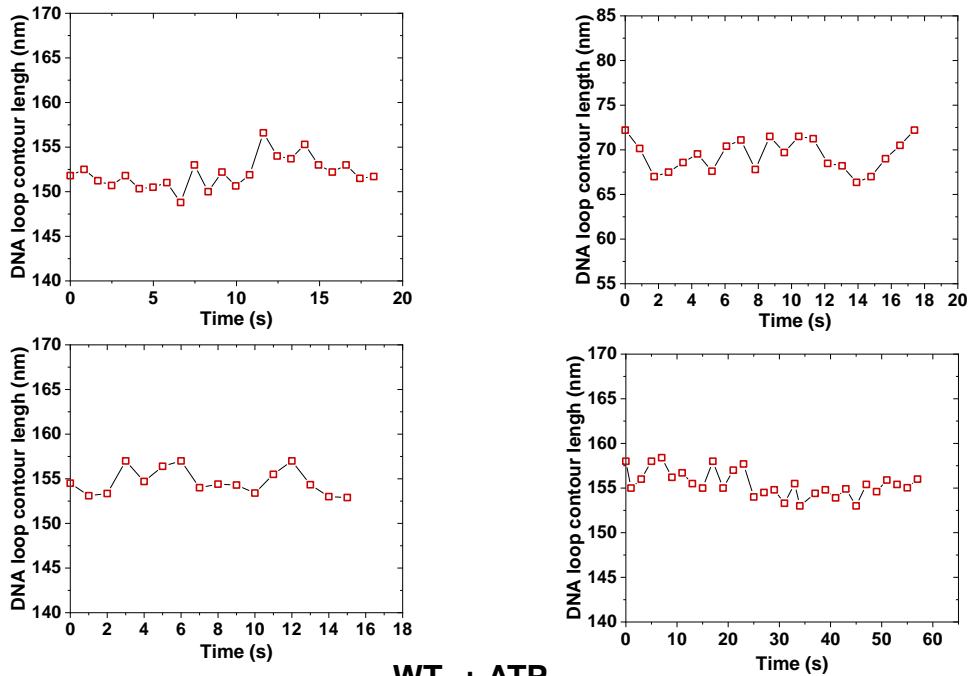
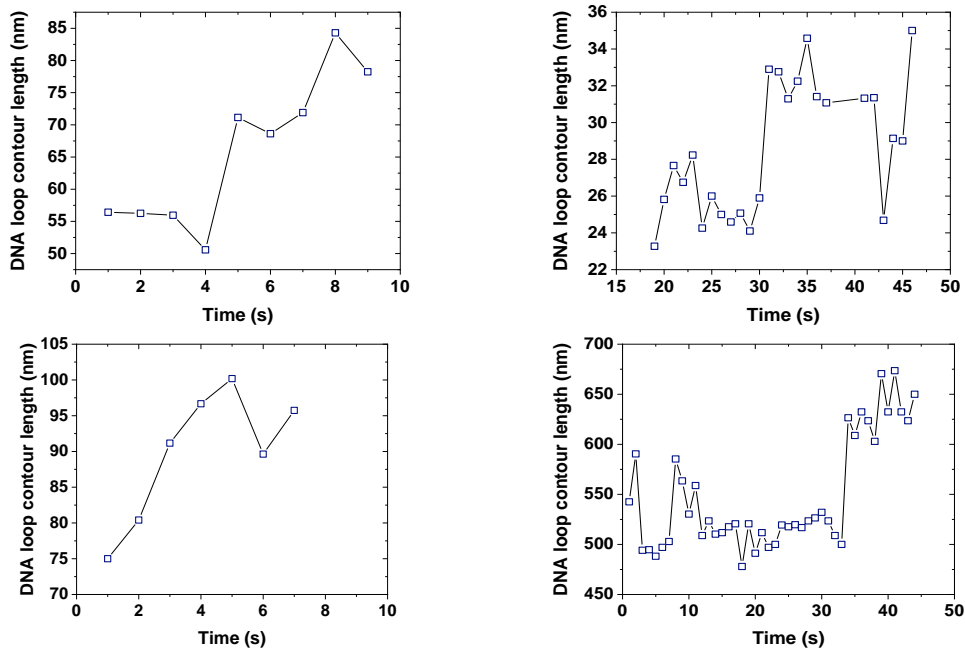
A**ATPase mutant + ATP****B****WT + ATP**

Figure S8. DNA loop length changes mediated by the ATPase mutant and WT cohesin^{SA1}-NIPBL^c on linear dsDNA in the presence of ATP . A, Frame-to-frame DNA loop lengths versus time for four independent DNA loops mediated by the cohesin^{SA1}-NIPBL^c ATPase mutant (4 mM ATP). B, Additional examples of frame-to-frame DNA loop lengths versus time mediated by WT cohesin^{SA1}-NIPBL^c (4 mM ATP).

```

NIPBL_HUMAN 2667 T E D D E S D G E D R G ---GGT S G S L R R S K R N S D S T E L A A Q M N E S V D V M D V I A I C C P K Y K D R P Q I A R V V Q K T S S G F S V Q W M A G S 2743
NIPBL_MOUSE 2661 T E D E E S D G E D R G ---GGT S G S L R R S K R N S D S T E L A A Q M N E S V D V M D V I A I C C P K Y K D R P Q I A R V V Q R T S S G V S V Q W M A G S 2737
NIPBL_XENLA 2813 T E E E E S D G E E K A ---GGT S G - L R K S K R L S D S S D V A V Q M N E T V D V Q D V I A I C S P K Y K D R P Q I A K V V Q K T S H G L S I R W M A G S 2888
NIPBL_DANRE 2743 Y D D D - S E V E - - - - - E K T P G S S R R S R R T G D S A E A S G H R N E T V E A T D V I A L C C P K Y K D R P Q I A R V I Q K T S K G Y S I H W M A G S 2815
NIPBL_DROME 2010 S S - - - - - - - - - - - - - A K N S H S A C D G - - - - - - - Y S L T V T D V V D V P M S H - - - - - I A K A S M - - - - - - - L T S K 2046

NIPBL_HUMAN 2744 Y S G S W T E A K - - R R D G R K L V P W V D T I K E S D I I Y K K I A L T S . K V V Q T L R S L Y A A K D G T S S 2804
NIPBL_MOUSE 2738 Y S G S W T E A K - - R R D G R K L V P W V D T I K E S D I I Y K K I A L T S . K V V Q T L R S L Y A A K D G T S S 2798
NIPBL_XENLA 2889 Y S G T W A E A K - - R R D G R K L V P W V D T I K E S D I I Y K K I A L T S A N K L T N K V A Q T L R S L Y A A K D G T S S 2949
NIPBL_DANRE 2816 Y S G T W A E A K - - R R D G R K L V P W V D T I K E S D I I Y K K I A L T S A H K L S N K V V Q T L R S L Y A A K E G S S S 2876
NIPBL_DROME 2047 P S G R K T N P V R T K K K R R K I D S T D D - - E T S D A E Y A - - - - - - - - - - - - - - - - - - - - - - - 2077

```

Figure S9. The C-terminal domain of NIPBL contains conserved positively charged residues. Alignment of sequences at the C-terminus of NIPBL from different species. Positively charged residues are highlighted in blue.